

# Supersymmetry without a light Higgs boson at the LHC

Leone Cavicchia, Roberto Franceschini, Vyacheslav S. Rychkov

*Scuola Normale Superiore and INFN, Piazza dei Cavalieri 7, I-56126 Pisa, Italy*

## Abstract

We analyze the LHC phenomenology of  $\lambda$ SUSY — a version of NMSSM with a largish  $SH_1H_2$  coupling. The scalar spectrum of the model contains a  $200 - 300$  GeV Higgs boson  $h$  with Standard-Model like properties, and heavy CP-even and CP-odd Higgs bosons  $H$  and  $A$  with masses in  $500 - 800$  GeV range. We study the discovery potential of  $H$  and  $A$  in the decay chains  $H \rightarrow hh \rightarrow 4V \rightarrow 2l6j$  and  $A \rightarrow Zh \rightarrow Z2V \rightarrow 2l4j$ . The dominant backgrounds are the diffuse  $Z6j$  and  $Z4j$  productions, which can be suppressed by demanding reconstruction of  $V$ 's and  $h$ 's in intermediate states. The excess of signal events allows for a discovery of both  $H$  and  $A$  with over  $5\sigma$  significance for  $100 \text{ fb}^{-1}$  of integrated luminosity.

# 1 Introduction

The Naturalness problem of the Electroweak scale amounts to explaining the relative lightness of the Higgs boson compared to the Ultra-Violet (UV) cutoff of the theory. It is important to stay focused on this problem, since it provides the best hope to see new physics at the LHC. The scale of this new physics crucially depends on the mass of the Higgs boson: the lighter the Higgs boson, the lower this “naturalness cutoff” is expected to be.

To make a quantitative estimate, one can use the indirect information contained in the ElectroWeak Precision Tests (EWPT). The Standard Model (SM) successfully accounts for the EWPT results for the Higgs boson mass  $m_h = 76^{+33}_{-24}$  GeV [1] at 65% C.L. The standard interpretation of this fact is that  $m_h$  should be quite close to its LEP2 direct lower bound of 114 GeV. To make such a light Higgs boson natural, new physics cutting off the top quark loop divergence should come in at or below the scale  $\Lambda_{\text{nat}} \simeq 400\sqrt{\Delta}$  GeV, if one allows finetuning of one part in  $\Delta$ .

The above standard interpretation of the EWPT has in it an implicit assumption that the new physics, while cutting off the top (and gauge boson) loops, does not itself contribute to the EWPT parameters  $T$  and  $S$  in a significant way. This assumption is, however, questionable, especially because the dependence of  $T$  and  $S$  on  $m_h$  is quite weak (logarithmic) in the SM. For example, a small breaking of the custodial symmetry in the new physics sector could be enough to generate an extra positive contribution to  $T$  making a much heavier Higgs boson consistent with the EWPT. This in turn allows to raise the naturalness cutoff of the theory by a non-negligible amount. This scenario, dubbed “Improved Naturalness”, has been realized in simple explicit models [2] and leads to interesting modifications in the expected LHC phenomenology.

Supersymmetry (SUSY), in many respects the most appealing way to UV-complete the SM, has its own specific problem with the Higgs boson mass. In supersymmetric extensions of the SM valid up to the GUT scale, such as the Minimal Supersymmetric SM (MSSM), the lightest Higgs boson  $h$  is generically predicted to be not much heavier than the  $Z$ . To achieve  $m_h \geq 114$  GeV requires a large radiative correction from the heavy stop, which introduces a few percent finetuning in the  $Z$  boson mass. This “SUSY Little Hierarchy Problem” led to several attempts in the literature to increase  $m_h$  by considering extensions of MSSM with extra sources for the Higgs quartic coupling.

A representative example of these attempts is the Next-to-Minimal Supersymmetric SM (NMSSM), which contains a chiral singlet  $S$  interacting with the MSSM doublets  $H_i$  via a superpotential term

$$\lambda SH_1 H_2. \tag{1.1}$$

The Yukawa coupling  $\lambda$  contributes to the Higgs quartic coupling. Its maximal possible value is usually fixed by the requirement that it should stay perturbative up to the unification scale  $\sim 10^{16}$  GeV, in order not to disrupt the gauge coupling unification, which gives  $\lambda_{\text{max}} \simeq 0.8$  at the electroweak scale [3]. The resulting extra contribution to  $m_h$  helps to bring it above the LEP2 bound, somewhat reducing the needed finetuning [4]. However, the conclusion that  $m_h$  should not be much above 114 GeV remains unchanged. In fact this conclusion seems quite generic in most<sup>1</sup> extensions of MSSM which assume that all extra couplings stay perturbative up to the unification scale [6], [7].

---

<sup>1</sup>A notable exception is [5].

On the other hand, if one abandons this assumption,  $m_h$  can be easily increased to a few hundreds of GeV. The most straightforward way to do this is based on adding the same term (1.1) to the superpotential, and taking  $\lambda$  large. The scale  $\Lambda_{\text{strong}}$  at which  $\lambda$  becomes non-perturbative can be interpreted as the compositeness scale of (some of) the scalars, and the superpotential (1.1) can appear as an effective low-energy description of a confining SUSY gauge theory UV-completing the model above  $\Lambda_{\text{strong}}$ .

The early studies of this idea [8]<sup>2</sup>, which we call  $\lambda$ SUSY to emphasize the role played by  $\lambda$ , have shown that such UV-completions do exist and, moreover, can be made consistent with the gauge coupling unification. This positive existence proof is important in convincing us that  $\lambda$ SUSY should be taken seriously. However, the details of the UV-completion are largely irrelevant for the TeV-scale phenomenology of the model, whose unique features are mostly determined by the presence of the large coupling  $\lambda$  in the superpotential.

Recently, the phenomenology of  $\lambda$ SUSY, with the focus on the key issue of the EWPT, has been closely examined in [9]<sup>3</sup>, and a very encouraging picture has emerged. Assuming that  $\lambda$  remains perturbative up to about 10 TeV<sup>4</sup>, the lightest Higgs boson can be in 200 – 300 GeV range and yet consistent with the EWPT because of the extra positive contributions from the Higgs/Higgsino sector to the T parameter. These extra contributions are governed by the same coupling  $\lambda$  as the Higgs mass, and thus do not require unnatural finetuning for cancellation. As a consequence of the increase in  $m_h$ , superpartners such as stop can be in 500 – 1000 GeV range without finetuning ( $\Delta = 5$ ). This is the supersymmetric counterpart of the Improved Naturalness.

Another attractive feature of  $\lambda$ SUSY is the possibility of Higgsino Dark Matter. Due to strong mixing in the Higgsino sector induced by the same large  $\lambda$ , the lightest Higgsino annihilation cross section is reduced compared to the MSSM case, and the observed Dark Matter abundance is reproduced in a large part of the parameter space [9].

All of the above makes  $\lambda$ SUSY a well-motivated alternative to the conventional SUSY scenario. In this paper we would like to continue the study of  $\lambda$ SUSY, focusing on its LHC phenomenology. Our purpose is twofold: we want to depict an LHC scenario which is impossible for conventional SUSY, but very natural for  $\lambda$ SUSY, and we want to analyze how  $\lambda$ SUSY could be observed at the LHC. We begin in Section 2 with a review of the model [9], stressing the differences with MSSM and NMSSM-like theories. In Section 3, we describe the early-stage LHC phenomenology of  $\lambda$ SUSY, rather puzzling from the point of view of more standard SUSY scenarios. This puzzle would beg for an explanation and extra evidence, and we argue that it could come from observing the peculiar heavy scalars of the model. Our main result is a detailed study of the LHC discovery potential in the scalar sector of  $\lambda$ SUSY at 100 fb<sup>-1</sup> of integrated luminosity (Sections 4, 5). We summarize our conclusions in Section 6.

---

<sup>2</sup>Originally called ‘Supersymmetric Fat Higgs’.

<sup>3</sup>See also [10], where however the important Higgsino contributions to the EWPT have not been included.

<sup>4</sup>This is necessary so that the EWPT can be analyzed in a fully perturbative way.

## 2 Review of $\lambda$ SUSY model

The field content of  $\lambda$ SUSY is the same as that of the NMSSM; that is, the only new field compared to the MSSM is a chiral singlet superfield  $S$ . The key feature of the model is the presence of the superpotential interaction (1.1) with a large coupling  $\lambda$ , which increases the mass of the lightest Higgs boson and improves naturalness of the theory, allowing for heavier superpartners. The maximal value of  $\lambda$  is limited by the assumption that it stays perturbative up to about 10 TeV, so that the in calculable contribution to the EWPT from the cutoff can be neglected. In this paper, just as in [9], we take  $\lambda = 2$  at the electroweak scale. For this value of  $\lambda$  the Landau pole is at about 50 TeV, which can be interpreted as the compositeness scale of (some of) the Higgs bosons [8].

### 2.1 Scalar sector

The full  $\lambda$ SUSY superpotential is

$$W = \mu(S)H_1H_2 + f(S), \quad \lambda = \mu'(S),$$

while the scalar potential can be written in the form

$$V = \mu_1^2(S)|H_1|^2 + \mu_2^2(S)|H_2|^2 - (\mu_3^2(S)H_1H_2 + \text{h.c.}) + \lambda^2|H_1H_2|^2 + V(S). \quad (2.1)$$

Here we neglected the gauge D-term contributions to the quartic term, which are small compared to the superpotential contribution for the chosen value of  $\lambda$ .<sup>5</sup> The mass parameters of the potential also include contributions from the soft SUSY-breaking Lagrangian. For simplicity, we assume CP invariance of  $V$  and  $W$ .

Many of the phenomenologically relevant properties of  $\lambda$ SUSY can be characterized by the functions  $\mu_i^2(S)$ ,  $\mu(S)$ , and  $M(S) = f''(S)$  evaluated at the Vacuum Expectation Value (VEV)  $s$  of the field  $S$ . These background values will be denoted below as  $\mu_i^2, \mu$  and  $M$  leaving their argument  $s$  understood. For example, the electroweak symmetry breaking (EWSB) is described by the equations

$$\begin{aligned} \tan \beta &\equiv \frac{v_2}{v_1} = \frac{\mu_1}{\mu_2}, \\ \lambda^2 v^2 &= \frac{2\mu_3^2}{\sin 2\beta} - \mu_1^2 - \mu_2^2, \end{aligned} \quad (2.2)$$

where  $v_{1,2}$  are the VEVs of the Higgs fields ( $v \equiv (v_1^2 + v_2^2)^{1/2} = 175$  GeV). The mass of the charged Higgs bosons  $H^\pm$  is

$$m_{H^\pm}^2 = \mu_1^2 + \mu_2^2.$$

The masses of the light neutral scalars can also be expressed via  $\mu_i^2$  if their mixing with  $S$  can be neglected (we will comment about the validity of this approximation below). The mass of the

---

<sup>5</sup>E.g., the D-terms increase the mass of the lightest Higgs boson of the model by 5 – 10 GeV compared to the expressions given below.

pseudoscalar  $A$  is then given by

$$m_A^2 = \frac{2\mu_3^2}{\sin 2\beta} = m_{H^\pm}^2 + \lambda^2 v^2.$$

The CP-even states  $h_i$  have mass matrix

$$\begin{pmatrix} m_A^2 \sin^2 \beta & (\lambda^2 v^2 - \frac{1}{2} m_A^2) \sin 2\beta \\ (\lambda^2 v^2 - \frac{1}{2} m_A^2) \sin 2\beta & m_A^2 \cos^2 \beta \end{pmatrix}.$$

The masses and compositions of the mass eigenstates  $h, H$  are given by:

$$\begin{aligned} m_{H,h}^2 &= \frac{1}{2}(m_A^2 \pm X), \quad X^2 = m_A^4 - 4\lambda^2 v^2 m_{H^\pm}^2 \sin^2 2\beta, \\ H &= \cos \alpha h_1 + \sin \alpha h_2, \quad h = -\sin \alpha h_1 + \cos \alpha h_2, \\ \tan \alpha &= \frac{m_A^2 \cos 2\beta + X}{(\lambda^2 v^2 - m_{H^\pm}^2) \sin 2\beta}. \end{aligned} \tag{2.3}$$

It is convenient to parametrize the scalar sector of the model in terms of two parameters:  $\tan \beta$  and  $m_{H^\pm}$ . Their preferred range is:

$$\begin{aligned} 1.5 &\lesssim \tan \beta \lesssim 3, \\ 350 \text{ GeV} &\lesssim m_{H^\pm} \lesssim 700 \text{ GeV}. \end{aligned} \tag{2.4}$$

Here the bounds on  $\tan \beta$  are suggested by the EWPT analysis [9]; the lower bound on  $m_{H^\pm}$  follows from requiring consistency with the constraint from  $b \rightarrow s\gamma$  without a destructive contribution from a stop-chargino loop [11]; the upper bound on  $m_{H^\pm}$  was derived in [9] from Naturalness considerations. The masses of neutral scalars in this range of parameters are given in Figs. 1,2. The key feature of the spectrum is that the lightest Higgs boson  $h$  is in the 200 – 300 GeV range, hence typically much heavier than in MSSM or NMSSM. Another notable feature (see Fig. 2) is the fixed ordering of the spectrum:

$$m_h < m_{H^\pm} < m_H < m_A.$$

Throughout the paper we will assume that the singlet scalar  $S$  is significantly heavier than  $H^\pm, H, A$ , and neglect the mixing between the neutral components of the Higgs doublets and the real and imaginary components of  $S$ . In fact  $S$  can be as heavy as 1 TeV or more, consistently with Naturalness [9]. In this case the no-mixing approximation works reasonably well. Analysis of concrete examples shows that the decrease in the masses of  $h, H, A$  due to their mixing with  $S$  does not typically exceed 5 – 10 %. At the same time the singlet admixture in  $h, H, A$  stays below 0.2 – 0.3.

## 2.2 Higgsino/Singlino sector

In the fermion sector of  $\lambda$ SUSY, we will assume that the electroweak gauginos are heavy and we will neglect their mixing with the Higgsinos. This is justifiable since the Higgsinos are mixed with

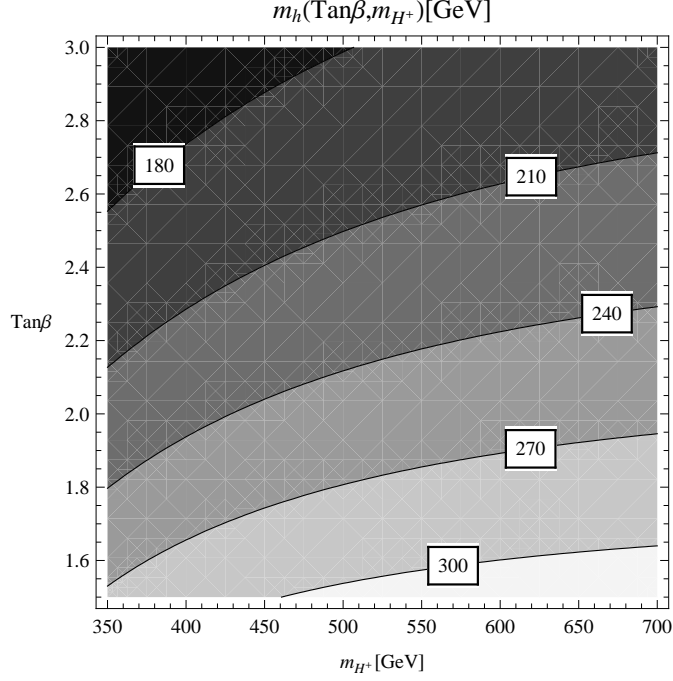


**Figure 1:** The mass of the lightest CP-even scalar  $h$  in the preferred region (2.4) of the parameter space. The coupling  $\lambda$  is fixed at  $\lambda = 2$ .

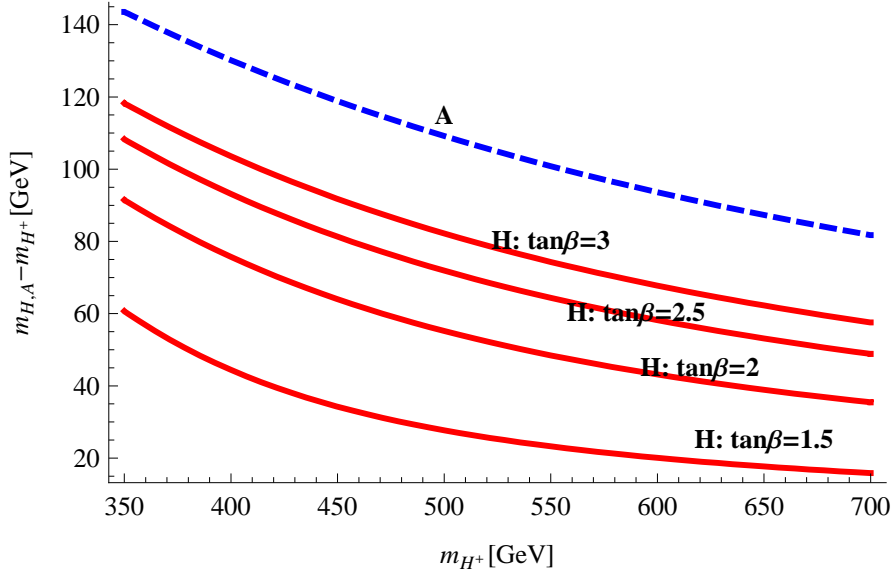


**Figure 2:** The second CP-even scalar  $H$  and the CP-odd scalar  $A$  are always heavier than the charged scalars  $H^\pm$ . This plot shows mass differences  $m_H - m_{H^\pm}$  (solid red lines,  $\tan \beta = 1.5, 2, 2.5, 3$  from below up) and  $m_A - m_{H^\pm}$  (dashed blue line) as a function of  $m_{H^\pm}$  in the preferred region (2.4) of the parameter space. The coupling  $\lambda$  is fixed at  $\lambda = 2$ .

the Singlino  $\tilde{S}$  by terms proportional to  $\lambda$ , while mixing with the gauginos are controlled by the relatively small gauge terms [9]. In this case the charged Higgsino  $\chi^+$  has mass  $\mu$ . The neutral Higgsino mass matrix depends on  $\mu$  and  $M$ ; its expression is given in [9]. The lightest neutralino is always lighter than the chargino:

$$m_{\chi_1^0} \leq m_{\chi^\pm} . \quad (2.5)$$

Stability of the potential gives an upper bound for the chargino mass:

$$m_{\chi^\pm} \leq \cos \beta m_{H^\pm} , \quad (2.6)$$

which in turn implies that the lightest neutralino typically has a mass in 100 – 200 GeV range, so that it is the Lightest Supersymmetric Particle (LSP). Interestingly, this lightest neutralino can play the role of Cold Dark Matter. This is in contrast with the MSSM, where the pure Higgsino Dark Matter is disfavored since it (co)annihilates very efficiently and typically gives too low thermal abundance [12]. In  $\lambda$ SUSY, the mixing between Higgsinos and the Singlino induced by  $\lambda$  allow to reduce the annihilation cross section and get the correct thermal relic abundance.

### 2.3 Other SUSY particles

The masses of the top squarks and of the gluino affect the running of  $\mu_2^2$  at the one- and two-loop level, respectively, and can thus be bounded from Naturalness considerations. For 20% finetuning ( $\Delta = 5$ ) and  $\tan \beta$  as in (2.4) these masses have to satisfy [9]

$$\begin{aligned} m_{\tilde{t}} &\lesssim 600 - 800 \text{ GeV} , \\ m_{\tilde{g}} &\lesssim 1.2 - 1.6 \text{ TeV} \end{aligned} \quad (2.7)$$

(looser bounds corresponding to smaller  $\tan \beta$ ). For larger finetuning  $\Delta$  these bounds increase by a factor  $\sqrt{\Delta/5}$ .

The masses of the electroweak gauginos, sleptons and all the other squarks except for the stops, do not have significant Naturalness bounds. Thus it is relevant to consider the limit when these particles are well above a TeV. This limit is similar to the models with effective supersymmetry [13], originally proposed as a way to address SUSY flavor problems.

## 3 $\lambda$ SUSY at the LHC

We will now discuss the LHC phenomenology of  $\lambda$ SUSY beginning from the easier signals of gluino, stop and the lightest Higgs and then continuing with a detailed analysis of the experimental signatures of the heavy scalars. In our discussion we will always assume  $\lambda = 2$  and  $\tan \beta$  and  $m_{H^\pm}$  belonging to the preferred range (2.4). More specific Monte Carlo studies will be performed for a benchmark point

$$m_{H^\pm} = 500 \text{ GeV}, \quad \tan \beta = 2 , \quad (3.1)$$

corresponding to light neutral scalar masses of

$$m_h = 250 \text{ GeV}, \quad m_H = 555 \text{ GeV}, \quad m_A = 615 \text{ GeV}.$$

### 3.1 Gluino and stop

The standard way to discover SUSY at the LHC is via pair-production of squarks and gluinos [22, 23]:

$$pp \rightarrow \tilde{g}\tilde{g}, \tilde{q}\tilde{q}, \tilde{q}\tilde{\bar{q}}.$$

Since these sparticles are strongly interacting, the production cross section can be as large as a pb or more depending on the masses [16]. The produced sparticles give rise to well-known cascade decays with lightest neutralinos in the final state, giving events with several jets, leptons and missing  $E_T$ .

The majority of available studies [22, 23] of this signal focus on the mSUGRA case, which gives degenerate squark spectra. While the same discovery strategy will apply also in the  $\lambda$ SUSY case, the discovery is expected to be more difficult due to the fact that only stop squarks may be light enough to be produced. For a rough estimate we can use the existing study [14] of the LHC discovery potential in the case of effective supersymmetry [13], when only the 1st and 2nd generation squarks are decoupled, while sbottom and stop masses are similar. Notice that in  $\lambda$ SUSY the LSP is expected to be relatively light with respect to the gaugino and stop (see Section 2.2), which helps the discovery. According to [14], in this favorable case  $10 \text{ fb}^{-1}$  of integrated luminosity should be enough for a discovery of SUSY in the entire range (2.7) of stop and gluino masses suggested by Naturalness.

The same signals with several jets, leptons and missing transverse energy can be used, in addition to SUSY discovery, to roughly estimate the sparticles masses. In fact, the total invariant mass of the visible particles in the final state cannot exceed the decaying sparticle mass. A concrete example is  $\tilde{t} \rightarrow llq\chi_0$ ; in this case one can set an upper bound on the stop mass

$$m_{\tilde{t}} > m_{llq}^{max},$$

where  $m_{llq}^{max}$  denotes the end-point of the invariant mass distribution of  $llq$ .

### 3.2 Light Higgs

The most peculiar property of the lightest Higgs boson  $h$  in  $\lambda$ SUSY is its mass (see Fig.1). This particle is always heavy ( $200 - 300 \text{ GeV}$ ), and this makes a relevant phenomenological difference with respect to the conventional supersymmetric models. To study other properties and analyze production and decay channels we need to know how the lightest Higgs interacts.

According to the standard 2 Higgs Doublet Model (2HDM) result, the couplings of the  $h$  with the top and the weak gauge bosons are equal to the coupling of the SM Higgs boson times the following factors:

$$\xi_{htt} = \frac{\cos \alpha}{\sin \beta}, \quad \xi_{hVV} = \sin(\beta - \alpha),$$

where from now on  $V$  means both  $Z$  and  $W$ . These are the only relevant couplings with SM particles. From Fig. 3 we see that the  $\xi_{htt}$  and  $\xi_{hVV}$  factors are very close to one (within 10%) in the whole parameter space of Eq. (2.4).

Since the  $h$  is SM-like, we expect the gluon fusion (GF) to be the dominant production process. For the moderate  $\tan \beta$  of Eq. (2.4) the bottom loop is always negligible with respect to the top



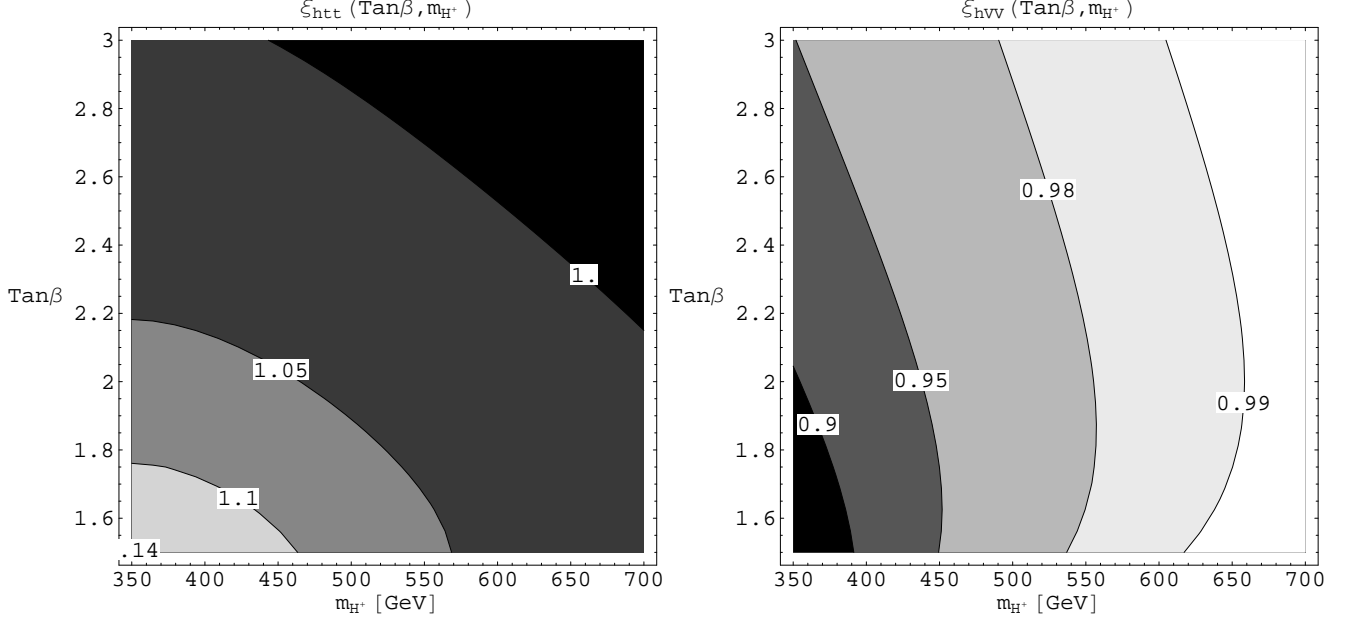


**Figure 3:**  $\xi_{htt}$  (left) and  $\xi_{hVV}$  (right), see Eq. (3.2), plotted in the range (2.4) for  $\lambda = 2$ .

loop. As discussed in Section 3.2.1 below, correction due to the stop loop is also quite small. We conclude that the GF production cross section of  $h$  is always close to the GF production cross section of the SM Higgs boson of the same mass.

On the other hand, decays of the  $h$  will also follow the same pattern as in the SM. In fact, the branching ratio is almost saturated by the decays into vectors. This allows to use existing SM Higgs boson studies to estimate the discovery potential of LHC. According to [22, 23],  $5\text{fb}^{-1}$  of integrated luminosity allows a  $5\sigma$  discovery in the “gold-plated” channel  $h \rightarrow ZZ \rightarrow l^+l^-l^+l^-$ . The mass of  $h$  will also be easily measurable thanks to good energy resolution of the final leptons: available studies [22, 23] report that  $30\text{fb}^{-1}$  will be enough to measure  $m_h$  at 1 – 2 ppm level.

### 3.2.1 Stop loop contribution to the GF production cross section

The full (top+stop) LO amplitude for GF production of  $h$  is given by:

$$\mathcal{A}_{\text{top+stop}}^h = g_{htt}A_{1/2}^h(\tau_t) + \sum_{i=1,2} \frac{g_{h\tilde{t}_i\tilde{t}_i}}{m_{\tilde{t}_i}^2} A_0^h(\tau_{\tilde{t}_i}), \quad \tau_i = \frac{m_h^2}{4m_{\tilde{t}_i}^2}. \quad (3.2)$$

Here  $\tilde{t}_i$  are stop mass eigenstates, and  $g_{h\tilde{t}_i\tilde{t}_i}$  are their couplings to the  $h$ . These depend on several parameters (stop soft masses  $m_Q, m_U, A_t$  as well as  $\mu, \alpha, \beta$ ) and are given by the same expressions as in the MSSM (see [21], p. 24, 39). The  $A_0^h$  and  $A_{1/2}^h$  are, respectively, the stop and top loop amplitude (see [21], p.92). At LO, the ratio of GF  $h$  production cross sections with and without

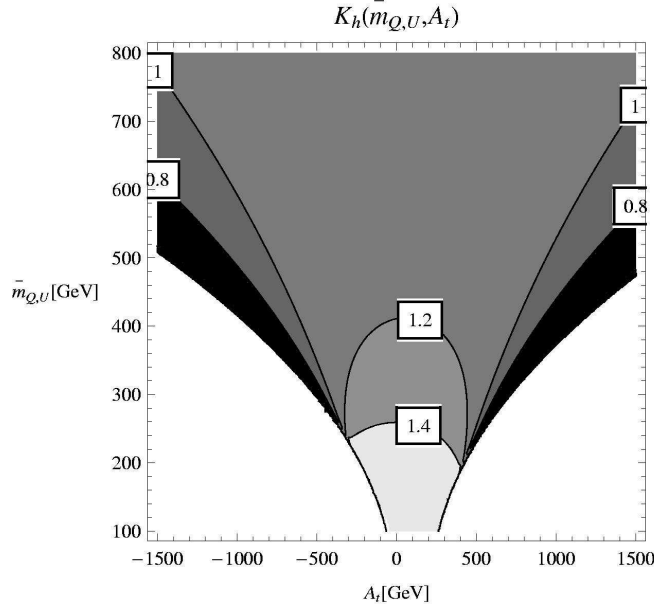


**Figure 4:**  $K_h$  plotted as a function of  $\bar{m}_{Q,U}$  and the top trilinear SUSY breaking term  $A_t$ . Other parameters are fixed as in Eq. (3.4). The white areas in the lower left and lower right corners correspond to  $m_{\tilde{t}_1} \leq 100$  GeV (see Fig. 6) and are therefore excluded by direct stop searches [15].

stop loop included is given by

$$K_h \equiv \frac{\sigma_{\text{top+stop}}}{\sigma_{\text{top}}} = \left| \frac{\mathcal{A}_{\text{top+stop}}^h}{\mathcal{A}_{\text{top}}^h} \right|^2, \quad (3.3)$$

where by  $\mathcal{A}_{\text{top}}^h$  we denote the first term in (3.2). To estimate the impact of the stop contribution, we evaluated  $K_h$  for various plausible values of stop sector parameters. For example, in Fig. 4 we give a plot of  $K_h$  as a function of  $\bar{m}_{Q,U} \equiv (m_U + m_Q)/2$  and  $A_t$ , with the other parameters fixed at

$$\tan \beta = 2, \quad m_{H^+} = 500 \text{ GeV}, \quad m_Q - m_U = 100 \text{ GeV}, \quad \mu = 200 \text{ GeV}. \quad (3.4)$$

As we can see from Fig. 4, inclusion of stop loops changes the GF  $h$  production cross section by a small amount (less than 20%). We have checked that this result remains unchanged for different choices of the parameters in (3.4). The stop contribution is thus of the same order of magnitude as the NNLO QCD correction to the top loop GF process.

### 3.3 What next?

The early discoveries described in the previous two sections, if they indeed happen at the LHC, will be somewhat puzzling. Strongly-interacting cascade-decaying heavy particles will give a strong evidence for SUSY. At the same time, a SM-like Higgs boson with a 200 – 300 GeV mass will rule

out the MSSM, or other conventional SUSY scenarios. Indeed, in the MSSM, the lightest Higgs boson mass has a theoretical upper bound of about 140 GeV <sup>6</sup>, and there is no way to make the model compatible with the phenomenology of Sections 3.1 and 3.2. The same conclusion holds for all the extensions of the MSSM which keep couplings perturbative up to the unification scale.

A natural way to resolve the puzzle is to allow couplings which become non-perturbative at a lower scale, and  $\lambda$ SUSY is the simplest model which realizes this idea. At this point it will become crucial to make further tests of the model. With this in mind, below we will study the discovery reach of heavy scalars  $H$  and  $A$  and their mass measurement. This will be probably the simplest non-trivial measurement to perform. Interestingly, by measuring  $m_H$  and  $m_A$  (and assuming that we have already measured  $m_h$ ), we can determine the main scalar sector parameters  $m_{H^\pm}$ ,  $\tan\beta$  and  $\lambda$  (see Section 2.1). Knowing  $\lambda$ , we can tell the scale at which compositeness/strong coupling sets in.

## 4 The heavy CP-even scalar @ LHC

### 4.1 Production

The heavy CP-even Higgs boson  $H$  (see Eq. (2.3)) has mass in the 500-800 GeV range (see Fig. 2). Its couplings to fermions and weak gauge bosons are equal to the couplings of the SM Higgs boson times the following factors (see Fig. 5):

$$\xi_{Htt} = \frac{\sin\alpha}{\sin\beta}, \quad \xi_{Hbb} = \frac{\cos\alpha}{\cos\beta}, \quad \xi_{HVV} = \cos(\beta - \alpha) .$$

The Higgs-stop coupling  $g_{H\tilde{t}_1\tilde{t}_1}$  is the same as in the MSSM and depends on  $\mu$ , the  $\alpha$  and  $\beta$  angles and on the top soft SUSY-breaking A-term  $A_t$  (see [21], pg. 24, 40 for explicit expressions).

The relevant production processes are GF and vector boson fusion. Both top and stop loop contribute to the GF cross section.<sup>7</sup> To estimate the relevance of stop contribution we studied the quantity  $K_H$ , defined analogously to  $K_h$  from Sec. 3.2. In Fig. 6 we plot  $K_H$  and  $m_{\tilde{t}_1}$  as functions of  $\bar{m}_{Q,U}$  and  $A_t$  with the other parameters fixed as in (3.4). From this picture we can see that: (a) in most of the allowed area stop contribution enhances the cross section; (b) in the area corresponding to

$$m_{\tilde{t}_1} > 400 \text{ GeV} \tag{4.1}$$

the stop loops correct the GF cross section by less than 20%. As in the light Higgs case, such a contribution is comparable to NNLO QCD correction to the top loop diagram, which is never taken into account in this paper. In what follows we will neglect the stop loop contribution to the  $H$  production. Thus, in most of the parameter space we will be *underestimating* the production cross section. In principle, as discussed in Section 3.1, stop mass is likely to be determined/constrained from cascade decays. Therefore we would be able to check assumptions like (4.1) and improve the accuracy for GF  $H$  production cross section prediction.

---

<sup>6</sup>Assuming  $m_{\text{stop}} \lesssim 2 \text{ TeV}$ , see [21].

<sup>7</sup>The bottom loop contribution can be safely neglected because  $\xi_{Hbb}$  is not large enough to make it comparable with the top loop for moderate  $\tan\beta$  as in (2.4).

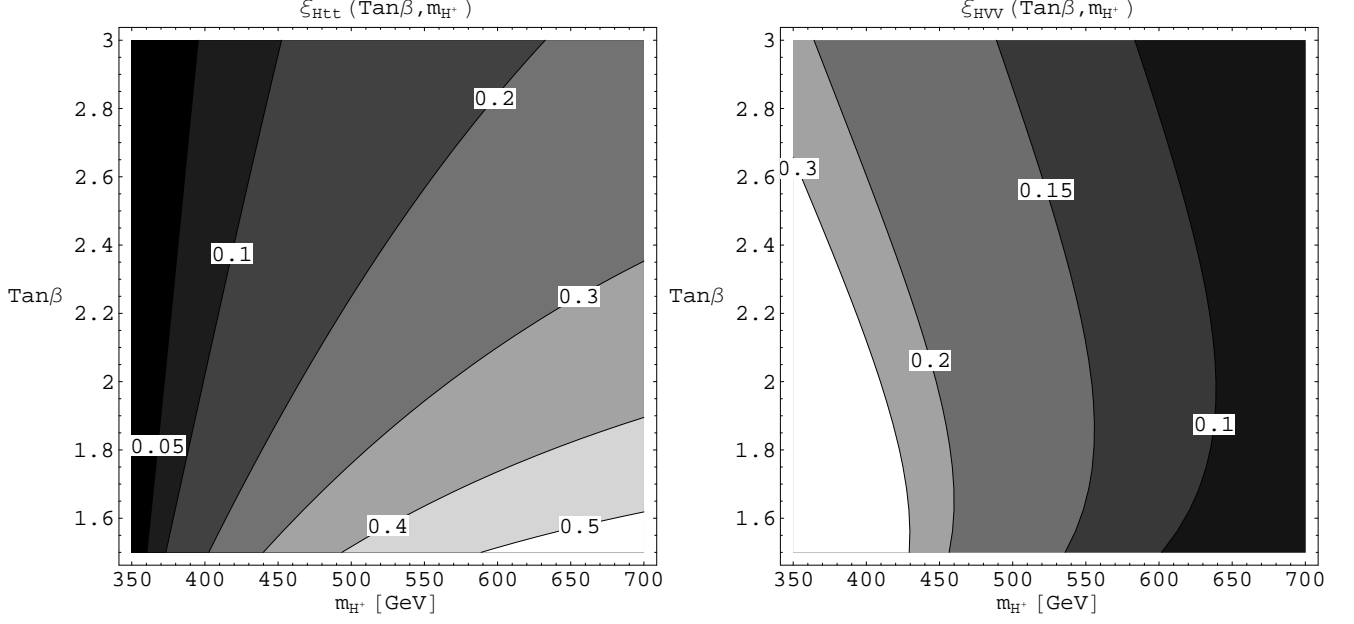


**Figure 5:**  $\xi_{Htt}$ (left) and  $\xi_{HVV}$ (right) plotted in the range (2.4) for  $\lambda = 2$ .

We thus obtain the gluon fusion (GF) and vector boson fusion (VBF) production cross sections of the  $H$  by simply rescaling the NLO results for the SM Higgs boson of the same mass, generated by HIGLU [17] and vv2H [18] codes. For instance the GF result is given by:

$$\sigma^{GF}(H) = \xi_{Htt}^2 \sigma_{SM}^{GF}.$$

The obtained production cross sections are shown in Fig. 7. With an order of 0.1 pb production cross section (GF being the dominant mode), the search for  $H$  looks feasible.

## 4.2 Decays

The visible decay width of the  $H$  is dominated by decays into  $hh$ ,  $t\bar{t}$  and  $VV$  pairs. We assume that the decay channel into a stop pair is closed, which happens in most of the parameter space (see Fig. 6); such an assumption can be checked and corrected if necessary when the stop mass is measured. The  $Hhh$  coupling is proportional to  $\lambda^2$  and is given by<sup>8</sup>

$$g_{Hhh} = \frac{v\lambda^2}{2\sqrt{2}} [\sin(\alpha + \beta) - 3\sin(3\alpha - \beta)].$$

The total visible decay width is given in Fig. 8 and ranges between 5 and 25 GeV. The branching ratio for decays into  $hh$  and, for comparison, into  $ZZ$  pairs, is plotted in Fig. 9. Because  $\lambda$  is large,

<sup>8</sup>The corresponding Lagrangian term is  $g_{Hhh}Hh^2/2$ .

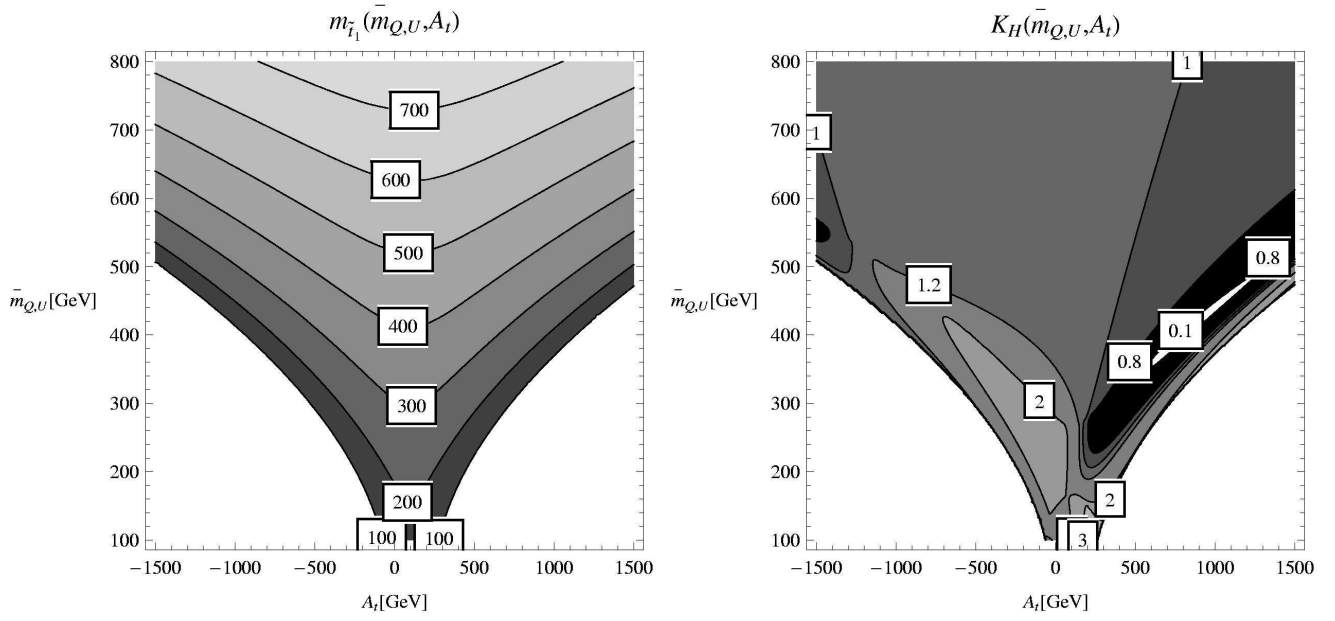


**Figure 6:** *Left:* mass of the lightest stop plotted as a function of  $\bar{m}_{Q,U}$  and  $A_t$ . *Right:* The  $K_H$  ratio plotted as a function of  $\bar{m}_{Q,U}$  and  $A_t$ . In both plots parameters are fixed as in Eq. (3.4). The white areas in the lower left and lower right corners correspond to  $m_{\tilde{t}_1} \leq 100$  GeV and are therefore excluded by direct stop searches [15].

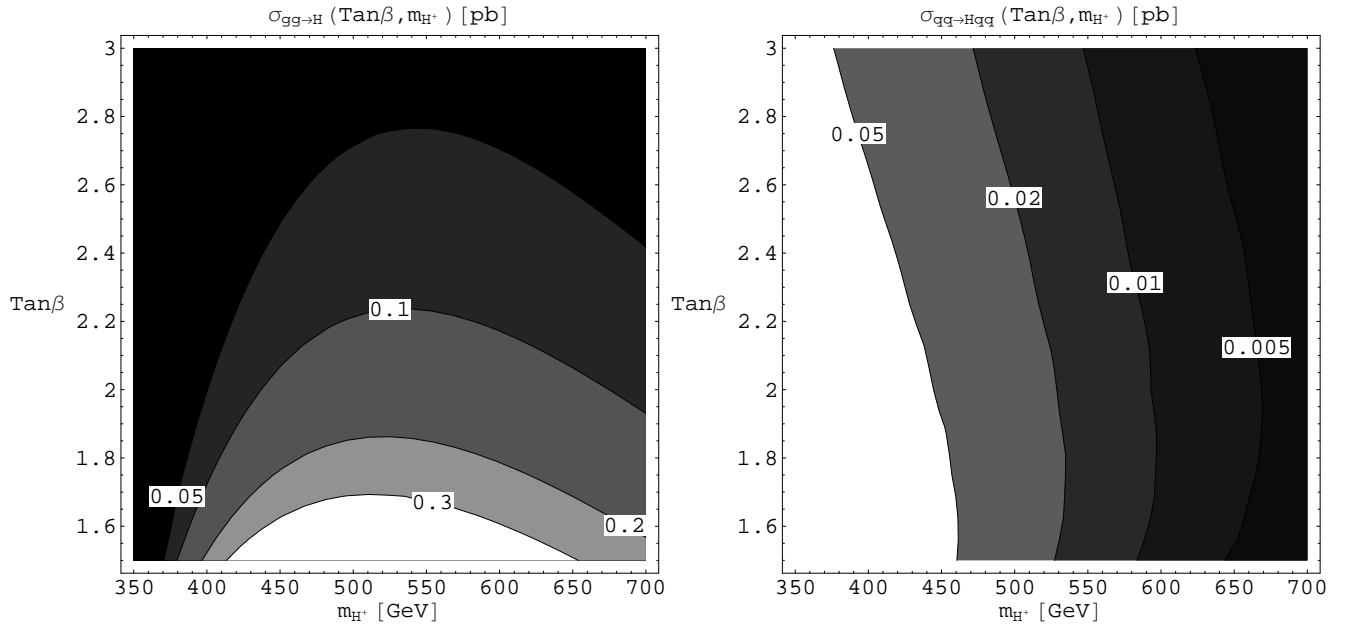


**Figure 7:** The NLO production cross section of the  $H$  via the gluon fusion (left) and the vector boson fusion (right) plotted in the range (2.4) for  $\lambda = 2$ .

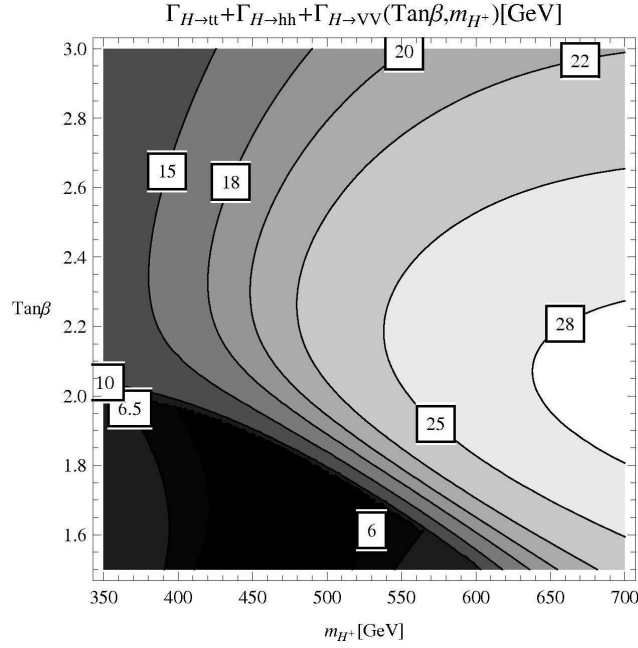


**Figure 8:**  $\Gamma_H$  omitting supersymmetric decays into Higgsino pairs, see Fig. 10.

decay into  $hh$  pairs is a dominant decay mode whenever this channel is open, which happens in most of the parameter space.

The  $H$  will also decay into Higgsino pairs. This decay width depends on the Higgsino sector parameters  $\mu$  and  $M$ , see Sec. 2.2. Fig. 10 gives the decay width of  $H$  into Higgsinos for the benchmark point (3.1) and for  $\mu$ ,  $M$  within their ranges (determined by stability of the potential and Naturalness considerations [9]): it takes values between a few and 15 GeV. Below we will neglect the decay width into Higgsinos. This means that in a realistic situation all branching ratios and signal rates will have to be multiplied by a factor  $\Gamma/(\Gamma + \Gamma_{\chi\chi})$ .

### 4.3 Detection strategies

Let us first discuss the lower left corner of the parameter space, where the  $H \rightarrow hh$  decay channel is closed (see Fig. 9). In this region  $BR(H \rightarrow VV)$  becomes significant. We believe that  $H$  could be discovered in this region via  $H \rightarrow ZZ \rightarrow 4l, \nu\nu ll$  combined with  $H \rightarrow WW \rightarrow l\nu l\nu$ . A rough estimate of the discovery reach can be obtained using results of the SM Higgs boson studies [22, 23], and then taking into account that the width of our  $H$  scalar is significantly smaller than the width of the SM Higgs boson of the same mass. More precisely, the discovery significance can be estimated by rescaling the corresponding significances in the SM case with a factor

$$\frac{(\sigma_H \times BR)_{\lambda SUSY}}{(\sigma_H \times BR)_{SM}} \sqrt{\frac{\Gamma_{SM}}{\Gamma_H}}$$

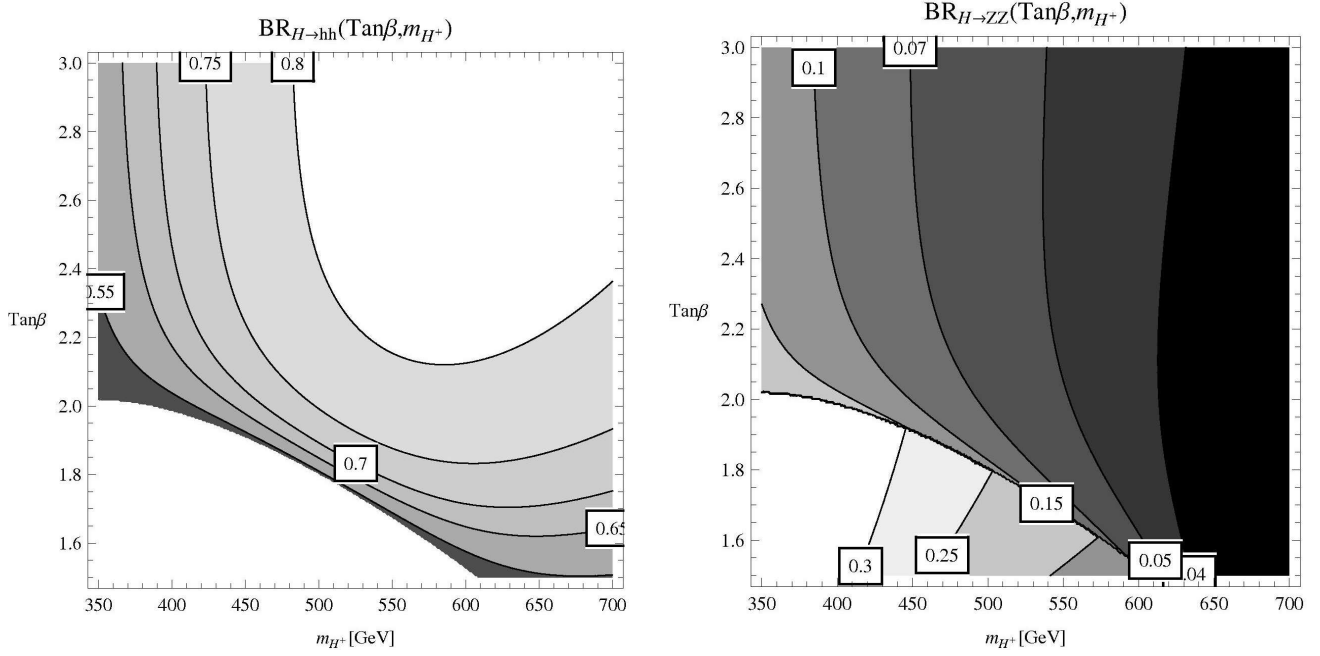


**Figure 9:**  $BR(H \rightarrow hh)$  (left) and  $BR(H \rightarrow ZZ)$  (right) in the preferred range (2.4) of the parameter space. The  $H$  decay width into Higgsinos  $\Gamma_{\chi\chi}$  is neglected. For nonzero  $\Gamma_{\chi\chi}$ , these branching ratios have to be multiplied by a factor  $\Gamma/(\Gamma + \Gamma_{\chi\chi})$ , where  $\Gamma$  is the visible decay width plotted in Fig. 8. The  $H \rightarrow hh$  decay mode is dominant except for the lower left corner of the parameter space where this decay channel is closed ( $m_H < 2m_h$ ).

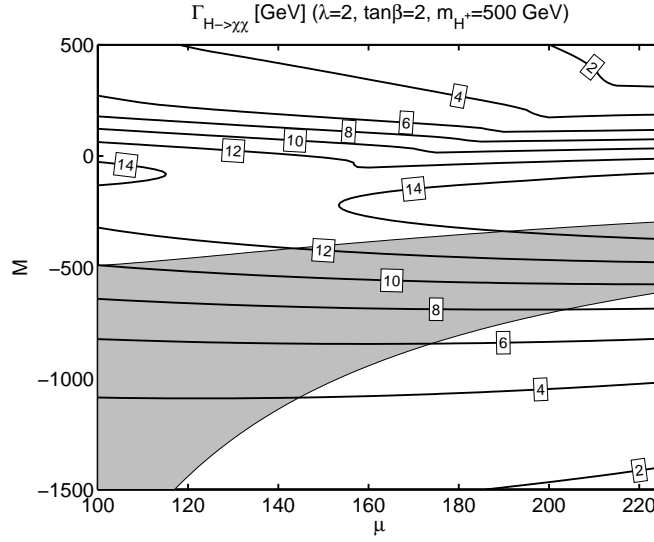


**Figure 10:** The  $H$  decay width into Higgsino pairs for  $\lambda = 2$ ,  $m_{H^+}$  and  $\text{tan}\beta$  at the benchmark point (3.1), and for  $\mu$  (chargino mass) and  $M$  within their ranges determined by stability of the potential and Naturalness considerations [9]. The gray area corresponds to  $m_{\text{LSP}} < m_Z/2$  and is excluded.

where the quantities marked by SM refer to the SM Higgs boson of the same mass as the  $H$ . The factor  $\sqrt{\Gamma_{SM}/\Gamma_H}$  reflects the reduction of background events passing the event selection in the mass window  $\pm \text{const.}\Gamma$ . This rescaling procedure gives a  $5 - 6\sigma$  significance with  $100 \text{ fb}^{-1}$  for the  $H$  discovery in  $H \rightarrow VV$  when  $H \rightarrow hh$  is closed<sup>9</sup>.

In the remaining, larger region of the parameter space,  $BR(H \rightarrow VV)$  is too small for a convincing  $H$  discovery in the  $VV$  decay channel. In what follows, we will discuss how  $H$  could be discovered in that region using the decay mode  $H \rightarrow hh$ . The fact that this decay mode is dominant when open reflects a very basic property of  $\lambda$ SUSY: the large value of  $\lambda$ .

## 4.4 Signal from $H \rightarrow hh$

For  $H \rightarrow hh$  decay we cannot rely on existing SM studies. To perform a careful analysis, we will consider a benchmark point (3.1). This point is generic rather than chosen for some special properties. The relevant particle parameters at this point take the following values<sup>10</sup>:

$$\begin{aligned} \sigma_H^{GF} &= 150 \text{ fb}, & \sigma_H^{VBF} &= 27 \text{ fb}, \\ m_H &= 555 \text{ GeV}, & m_h &= 250 \text{ GeV}, \\ \Gamma_H &= 21 \text{ GeV}, & \Gamma_h &= 3.8 \text{ GeV}, \\ \xi_{Htt}^2 &= 0.058, & \xi_{HVV}^2 &= 0.060, \\ BR(H \rightarrow hh) &= 0.76, & BR(H \rightarrow VV) &= 0.2. \end{aligned} \tag{4.2}$$

As discussed in Section 4.1, the  $H$  is mainly produced via gluon fusion; in the following we will consider only this channel. Once produced, most of the  $H$ s will decay into  $hh$  and then into  $4V$ , resulting in  $\sigma_{gg \rightarrow H \rightarrow 4V} = 110 \text{ fb}$ . The final weak bosons can decay leptonically, but the branching fractions in this case are too small to allow more than one leptonic decay. Our choice for a quantitative study is the channel with one leptonic  $Z$  decay, with the remaining weak bosons decaying hadronically<sup>11</sup>:

$$gg \rightarrow H \rightarrow hh \rightarrow 2Z2V \rightarrow l^+l^-6J, \quad \sigma \times BR = 2.67 \text{ fb}. \tag{4.3}$$

To increase the signal cross section, we assumed that final state jets  $J$  are *generic jets*, i.e.  $J = j, b, c$ , where  $j$  is a usual gluon or light-quark jet. Flavor labels are not necessary, since we will not deal with flavor tagging issues at all.

To produce a sample of signal events, we first used MADGRAPH [24] to produce matrix-element-generated  $gg \rightarrow H \rightarrow VVZl^+l^-$  events, and then we simulated the decay of the remaining weak bosons through the DECAY routine by F. Maltoni [24].

---

<sup>9</sup>The preceding discussion used the gluon fusion production mechanism. This result can presumably be improved using vector boson fusion, which is not normally used in the SM for this range of the Higgs mass, but becomes significant in  $\lambda$ SUSY for low  $m_{H^\pm}$  (see Fig. 7).

<sup>10</sup>The reported decay widths and branching ratios are calculated assuming zero decay widths into Higgsinos. See discussion in Section 4.2.

<sup>11</sup>The alternative channel  $H \rightarrow WWVV \rightarrow l\nu 6J$  benefits from a higher rate and could perhaps yield a higher statistical significance. Another promising channel is  $H \rightarrow WWWW$  with several same-sign or opposite sign-different flavor leptons in the final state, which was recently used in a related study of non-SUSY  $H \rightarrow hh$  decays [25]. We preferred channel (4.3) to avoid discussing additional sources of missing energy among which there are particularly delicate detector effects (jet energy scale, finite cone size effects, calibration, etc.).



## 4.5 Backgrounds

We scanned the long list of SM processes with  $l^+l^-6J$  final state and used ALPGEN[29] or MADGRAPH+DECAY to compute their cross sections for the total invariant mass near the  $H$  mass<sup>12</sup>. We found that only  $Z6J$  and  $t\bar{t}Z$  processes are relevant, i.e. have cross section large enough to potentially compete with the signal. The details of this preliminary analysis can be found in Appendix A.

We then proceeded with a more complete analysis of these two relevant backgrounds. Samples of  $(Z \rightarrow l^+l^-)6j$  and  $(Z \rightarrow l^+l^-)4jQ\bar{Q}$  ( $Q = c, b$ ) events were generated with ALPGEN using the CTEQ5L parton distribution functions (pdf). We used cuts

$$\begin{aligned} \Delta R_{JJ} > 0.7, \quad p_T^J > 20 \text{ GeV}, \quad \eta_J < 2.5, \\ 80 \text{ GeV} < m_{ll} < 100 \text{ GeV}, \quad \eta_l < 10. \end{aligned} \quad (4.4)$$

We also enforced the total invariant mass cut

$$400 \text{ GeV} < m_{tot,inv} < 2400 \text{ GeV}, \quad (4.5)$$

covering by a large margin the region near the  $H$  mass. This allows us to properly introduce a jet spectrum smearing and take into account possible effects from high invariant mass tails<sup>13</sup>. With these cuts, our results for the cross section are reported in Table 1. These results were obtained for the ALPGEN factorization and renormalization scale set at  $\mu_F^2 = m_Z^2 + p_{T,Z}^2$ . Our motivation for choosing this scale is twofold. First, the Tevatron experiments [30, 31] have confronted the observed rates of  $Z + N \text{ jets}$  events with ALPGEN simulations for various  $\mu_F^2$ , finding  $\mu_F^2$  values not far from our choice as best fitting the observations. Second, our  $\mu_F^2$  yields nearly the largest cross section we found trying out several possibilities available in ALPGEN. Thus we believe that the systematic uncertainty of background normalization is conservatively taken into account.

The  $(Z \rightarrow l^+l^-)t\bar{t}$  process, with subsequent  $6J$  decay of the  $t\bar{t}$  pair, was simulated with MADGRAPH+DECAY using the CTEQ6L1 pdf. We generated a sample using cuts (4.4) and setting the renormalization and factorization scale at  $\mu_F^2 = m_Z^2$ ; see Table 1 for the cross section estimate.

## 4.6 Analysis

The total background cross section, see Table 1, is much bigger than that of the signal, eq. (4.3). However, we expect signal events to have very specific structure due to the presence of intermediate resonances ( $h, W, Z$ ). Typical background events are not expected to have such structure and can be rejected by imposing *reconstruction cuts*, i.e. requiring that the intermediate state resonances be reconstructed by final state jets and leptons. This is the general idea of the analysis described below. The main issue is whether the rejection efficiency will be enough to sufficiently suppress the backgrounds.

---

<sup>12</sup>Possible SUSY backgrounds like sparticle mediated diffuse  $hh$  production and  $l^+l^-6J + LSP$  in gluino and squark decay have been estimated to be negligible.

<sup>13</sup>At the same time, the lower invariant mass cut in (4.5) was indispensable with our limited computer resources, since it improves greatly ALPGEN unweighting efficiency.

Process	specific cuts	$\sigma$
$(Z \rightarrow l^+l^-)6j$	—	1118(2) fb
$(Z \rightarrow l^+l^-)bb4j$	$p_T^l > 10$ GeV	94(2) fb
$(Z \rightarrow l^+l^-)c\bar{c}4j$	$p_T^l > 10$ GeV	92(1) fb
$(Z \rightarrow l^+l^-)(t\bar{t} \rightarrow 6J)$	$\eta_l < 2.5, p_T^l > 10$ GeV	5.86(2) fb

**Table 1:** Simulation of the relevant SM backgrounds for  $H \rightarrow l^+l^-6J$ . Apart from the shown specific cuts, all  $l^+l^-$  pairs and jets fulfill Eq. (4.4). Final state total invariant mass is between 400 and 2400 GeV except for  $Zt\bar{t}$ , which is produced without invariant mass restrictions.

The details of the analysis (performed with ROOT[26]) are as follows. First of all, our analysis is completely partonic, so neither showering nor jet reconstruction effects are taken into account. We also ignore flavor tagging and trigger issues, but our inclusive definition of jets and final selection cuts for leptons make these simplifications fully justified. However, in order to make the analysis more realistic, we do introduce a smearing of energies of individual jets using the expression

$$\frac{\sigma}{E} = \frac{0.5}{\sqrt{E/\text{GeV}}} + 0.03 \quad (4.6)$$

to generate the smearing coefficient, as prescribed in Table 9-1 of [28]<sup>14</sup>.

After smearing, we impose the kinematical cuts (4.4) on the jets and slightly tighten the corresponding leptonic cuts

$$\Delta R_{lJ} > 0.4, \quad p_T^l > 10 \text{ GeV}, \quad \eta_l < 2.5. \quad (4.7)$$

Background and signal events not passing these cuts are removed from the samples. The signal events passing these cuts correspond to the 0.42(1) fb cross section (to be compared with Eq. (4.3) without any kinematical cuts). The background cross sections are reduced by these tighter cuts only by a small amount compared to the values reported in Table 1.

Finally, we impose the *reconstruction cuts*, proceeding as follows<sup>15</sup>.

**R1.** For each event we try to group the 6 final jets into 3 pairs so that the jets in each pair *reconstruct* a W or a Z. By this we mean that the invariant mass  $m_{inv}$  of each pair has to satisfy the requirement:

$$M_V - \delta_V \leq m_{inv} \leq M_V + \delta_V, \quad \delta_V = 8 \text{ GeV}, \quad V \in \{W, Z\}.$$

In practice, the value of  $\delta_V$  cannot be taken too small because otherwise too many signal events will be rejected. The given value was motivated by the finite resolution of the W and the Z peaks which is determined by their natural widths as well as by the energy resolution of the detector as taken into account by the smearing procedure described above.

<sup>14</sup>This is also the smearing adopted in the ATLFast++ detector simulator [27].

<sup>15</sup>Geometrical discrimination has been attempted too, but turned out not to be very helpful, since both signal and background result in a largely boosted system.

Process	$\sigma$
$H \rightarrow 6Jl^+l^-$	0.286(8) fb
$(Z \rightarrow l^-l^+)6j$	0.15(1) fb
$(Z \rightarrow l^-l^+)QQ4j$	0.028(3) fb
$(Z \rightarrow l^-l^+)(t\bar{t} \rightarrow 6J)$	0.022(1) fb

**Table 2:** Signal and background cross sections after imposing the reconstruction cuts. For  $ZQ\bar{Q}4j$  the given value is the sum over  $Q = b, c$ .

**R2.** If a grouping into jet pairs reconstructing a W or a Z each is found, we proceed to impose a further condition that two  $h$ 's be reconstructed by four jets from two of these three pairs, say pair 1 and 2, and by two jets of pair 3 and the two leptons. In this case the precise reconstruction cut that we used is

$$m_h - \delta_h \leq m_{pair_1+pair_2} \leq m_h + \delta_h, \quad \delta_h = 18 \text{ GeV},$$

$$m_h - \frac{\delta_h}{\sqrt{2}} \leq m_{pair_3+l+l^-} \leq m_h + \frac{\delta_h}{\sqrt{2}},$$

where  $m_{pair_1+pair_2}$  and  $m_{pair_3+l+l^-}$  are the invariant masses of the  $4J$  and  $2Jl^+l^-$  final states. The value of  $\delta_h$  is again motivated by the natural width of  $h$  (with an additional spreading caused by the jet energy resolution). We also check that the gauge boson reconstructed by the jets of pair 3 is a Z, while the two gauge bosons reconstructed by the jets of pairs 1 and 2 have the same type (both W or both Z).

If no grouping of 6 jets into 3 pairs satisfying both R1 and R2 can be found (we go over all combinations), the event is rejected, otherwise it is retained. The retained events show the expected intermediate state resonance structure of the signal.

We ran the reconstruction analysis on the signal sample and on each of the relevant background samples shown in Table 1. The signal and background cross sections *after the reconstruction cuts* are given in Table 2. For each sample the number of events which passed the reconstruction cuts was large enough so that the statistical uncertainty in determining the rejection efficiency is reasonably small<sup>16</sup>. In fact it is this statistical uncertainty (determined from the usual  $\sqrt{N}$  fluctuations of the number of events passing the reconstruction cuts) which underlies the errors for the cross sections quoted in Table 2.

Two basic conclusions are evident from Table 2. On the one hand, we see that for the chosen parameters  $\delta_{V,h}$  the reduction in the signal cross section from what we had after the kinematical cuts is reasonably small (from 0.42 to 0.28 fb). On the other hand, we see that the reconstruction cuts have huge effect on backgrounds, giving the rejection efficiency of about  $10^{-3}$ . The final background cross section is comparable to that of the signal, making the discovery possible.

Finally, in Figure 11 we show the distribution of the signal and the total background cross section versus the total invariant mass of the event.

---

<sup>16</sup>For example, we had 1059 events in the signal sample which passed all the cuts.

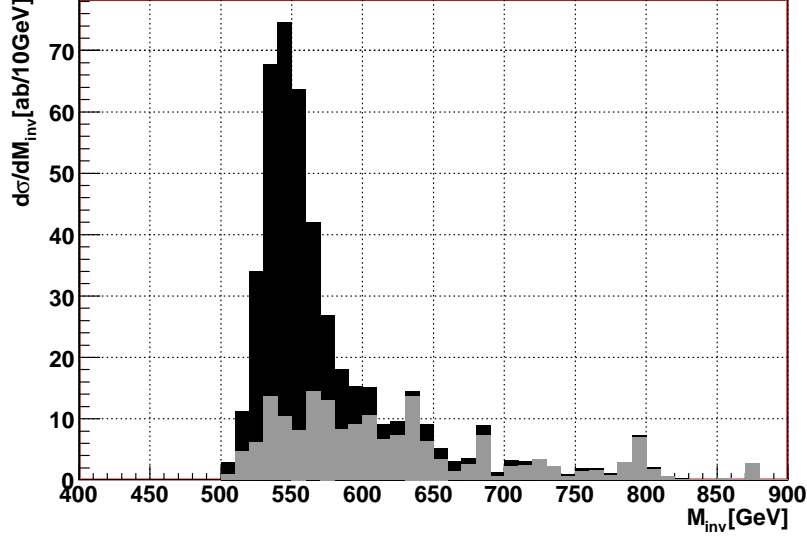


**Figure 11:**  $\lambda$ SUSY at the benchmark point (3.1), (4.2) (black) and Standard Model (grey) expectation for the differential cross section  $d\sigma/dM_{inv}(l^+l^-6J)$  after the kinematical and reconstruction cuts discussed in Section 4.6.

#### 4.7 Discovery potential after 100 fb<sup>-1</sup>

From Figure 11 we see that signal and backgrounds peak in the same invariant mass range. The discovery of  $H$  will thus come not from an observation of a new peak, but rather from an overall excess of events compared to the SM prediction, as well as from the enhanced prominence of the SM peak.

For an integrated luminosity of 100 fb<sup>-1</sup>, the expected number of events passing all the cuts is 20 in the SM, and 49 in  $\lambda$ SUSY at the benchmark point (3.1), (4.2), giving  $3.4\sigma$  if one uses the significance estimator formula given in Eq. (A.3) of [23]. Of course, once this global excess is found, it is worth to scan the invariant mass range to find where the excess is localized. Optimizing the range, much better discovery significance can be achieved. For instance, for 510 GeV <  $M_{inv}$  < 590 GeV we have 4 events in the SM, and 24 events in  $\lambda$ SUSY,  $6.86\sigma$  away from the SM. When going beyond benchmark-point analysis (something we do not attempt in this paper), such localized excess can be used to determine  $m_H$ .

Our conclusion is that the  $\lambda$ SUSY signal (4.3) is indeed observable at the LHC with 100 fb<sup>-1</sup> of integrated luminosity. If observed, it can provide clean evidence for the heavy scalar  $H$  as well as for the  $H \rightarrow hh$  dominant decay chain.

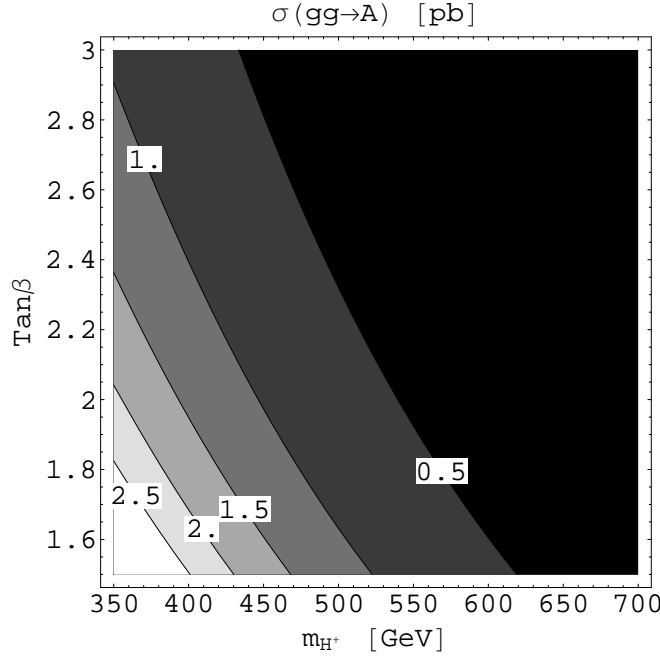


**Figure 12:** Pseudoscalar Higgs boson production cross section plotted in the parameter space of Eq. (2.4) for  $\lambda = 2$ .

## 5 The CP-odd scalar @ LHC

### 5.1 Production and decays

The pseudoscalar Higgs boson  $A$  has mass in the same 500-800 GeV range as the heavy scalar  $H$ , but is always heavier than  $H$  (see Fig. 2). Its couplings to the third generation SM fermions are given by [21]:

$$g_{Att} = \frac{m_t}{v} \cot \beta, \quad g_{Abb} = \frac{m_b}{v} \tan \beta.$$

There is also an  $g_{AhZ}(A \overleftrightarrow{\partial}_\mu h)Z_\mu$  coupling [21]

$$g_{AhZ} = \frac{g}{2 \cos \theta_w} \cos(\beta - \alpha),$$

where  $g$  is the SU(2) gauge coupling.

By CP-invariance  $AVV$  couplings vanish, therefore the only relevant production mechanism of  $A$  is gluon fusion. GF cross section is dominated by top loop. The bottom contribution is not significantly enhanced for moderate  $\tan \beta$  and remains negligible. Stop loops are absent due to the combined effect of CP, which forbids  $A\tilde{t}_1\tilde{t}_1$  and  $A\tilde{t}_2\tilde{t}_2$  couplings, and gauge invariance, which forbids gluon couplings to  $\tilde{t}_1\tilde{t}_2$  states.

The production cross section has been evaluated at NLO with HIGLU [17] and is plotted in Fig. 12.

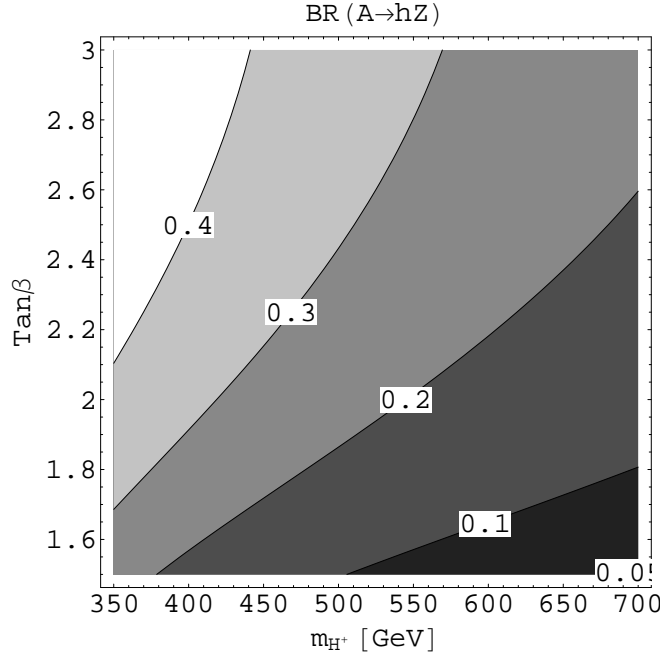


**Figure 13:**  $BR(A \rightarrow Zh)$  plotted in the parameter space of Eq. (2.4) for  $\lambda = 2$ , assuming negligible decay width into Higgsinos.  $BR(A \rightarrow t\bar{t}) \approx 1 - BR(A \rightarrow Zh)$ .

The total width of  $A$  ranges between 5 and 30 GeV and is dominated by  $A \rightarrow t\bar{t}$  and  $A \rightarrow hZ$  decays. Although the branching ratio of  $A \rightarrow t\bar{t}$  is almost always dominant (see Fig. 13), we cannot exploit this channel. Indeed, [19] showed that for the mass values we are interested in, the  $t\bar{t}$  SM background does not allow discovery of a scalar resonance decaying into  $t\bar{t}$ . Therefore, we focus on  $A \rightarrow hZ$ , whose BR is smaller, but still significant. Most of the produced  $h$ 's will decay into vectors, yielding  $\sigma_{tot}(gg \rightarrow A \rightarrow ZVV) \sim 100$  fb over all the parameter space. Such a cross section will give too small event rate if more than one  $V$  is allowed to decay leptonically. Therefore we concentrate on the signature

$$gg \rightarrow A \rightarrow hZ \rightarrow VVZ \rightarrow 4Jl^+l^- \quad (\text{signal}). \quad (5.1)$$

For a detailed study we go to our benchmark point (3.1), which gives the following numerical values<sup>17</sup>:

$$\begin{aligned} m_A &= 615 \text{ GeV}, & \Gamma_A &= 11 \text{ GeV}, \\ \sigma \times BR(\text{signal}) &= 6.9 \text{ fb}. \end{aligned} \quad (5.2)$$

<sup>17</sup>The quoted value of  $\Gamma_A$  does not include the width into Higgsino pairs depending on  $\mu$  and  $M$ . The latter can be as large as 10 GeV, but in most of the parameter space is below 2 GeV. See the analogous discussion for the  $H$  in Section 4.2.

Channel	$\sigma$
$A \rightarrow (Z \rightarrow l^+l^-)4J$	3.02(4) fb
$(Z \rightarrow l^+l^-)4J$	7.006(4) pb
$(Z \rightarrow l^+l^-)W2j$	176.0(8) fb
Sum of neglected	$\simeq 90$ fb

**Table 3:** Cross sections of the signal and of the relevant SM backgrounds after the kinematical cuts (5.3). Notice the reduction in the signal cross section compared to (5.2).

## 5.2 Analysis and discovery potential

The analysis is quite analogous to what was done in Section 4 for the heavy CP-even Higgs. We will therefore be relatively brief.

We generated a sample of signal events with MADGRAPH+DECAY.

We then computed cross sections for all SM processes with  $4Jl^+l^-$  final state and we found that only the  $Z4j$  and  $ZW2j$  processes are relevant<sup>18</sup>. Table 3 contains details about the relevant and neglected backgrounds.

Event samples of relevant backgrounds were generated for a more complete analysis. The  $Z4j$  process was simulated with ALPGEN using the CTEQ5L pdf, setting  $\mu_F^2 = m_Z^2 + p_{T,Z}^2$  and enforcing cuts:

$$\begin{aligned}
500 \text{ GeV} &< M_{inv} < 750 \text{ GeV} \\
p_T^j &> 20 \text{ GeV}, \quad p_T^l > 10 \text{ GeV}, \\
\Delta R_{jj, lj, ll} &> 0.4, \quad \eta^{j,l} < 2.5 \\
80 \text{ GeV} &< m_{ll} < 100 \text{ GeV}.
\end{aligned} \tag{5.3}$$

The  $ZW2j$  process was simulated with MADGRAPH using the CTEQ6L1 pdf, setting  $\mu_F^2 = m_Z^2$  and imposing the same cuts. The resulting background cross sections are the ones given in Table 3. Finally, to model finite detector energy resolution, we apply energy smearing to the signal and background events using the smearing function (4.6).

From Table 3 we see that the background cross section in the relevant interval of  $m_{inv}$  is more than 3 orders of magnitude above the signal. To reduce the background, we proceed by imposing the reconstruction cuts. Namely, we require that the 4 final jets can be divided into 2 pairs reconstructing a vector boson each. Moreover, we require that these two vector bosons be of the same type. If they are both W, then we require that they reconstruct an  $h$ . If they are both Z, we require that out of the 3 final Z's (the two from jets and the one reconstructed by the leptons) we should find two reconstructing an  $h$ . Reconstruction parameters  $\delta_{V,h}$ , having the same meaning as in Section 4.6, are taken to be

$$\delta_V = 8 \text{ GeV}, \quad \delta_h = 18 \text{ GeV}.$$

---

<sup>18</sup>In particular, backgrounds  $ZZ2j$ ,  $VVV$ ,  $h2j$  were analyzed and found negligible.

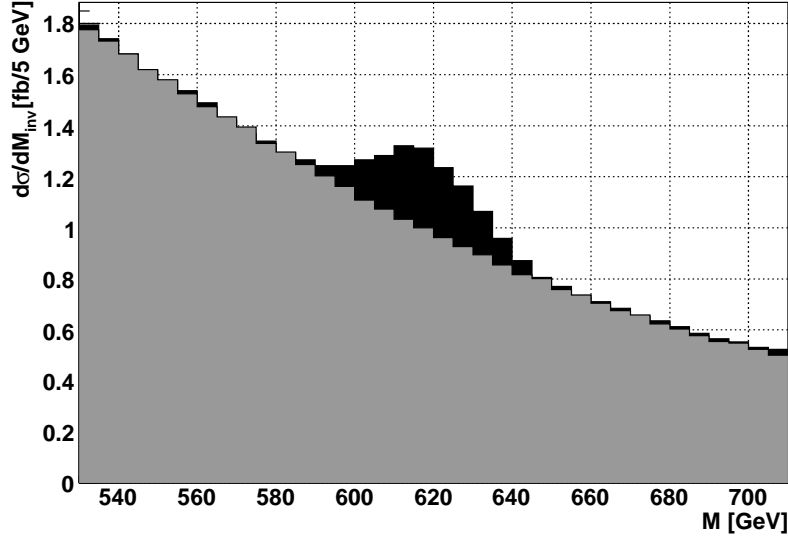


**Figure 14:**  $\lambda$ SUSY (black) and SM (grey) expected differential cross section  $d\sigma/dM_{inv}(4jl^+l^-)$  for process (5.1) at the benchmark point (3.1), (5.2).

If the above requirements can be satisfied, the event is retained, otherwise it is rejected.

The portion of the signal event sample which passes the reconstruction cuts amounts to 2.2 fb; cross section is reduced only by a small factor compared to the value after kinematical cuts given in Table 3. At the same time the total SM background cross section in 500 – 750 GeV invariant mass range drops after the reconstruction cuts by a factor of about 200, to 51.1 fb.

Of interest are the differential cross sections of background and signal+background versus the invariant mass, plotted in Fig. 14. We see that the signal distribution presents a clearly visible peak above the background. The discovery significance can be optimized choosing a range with largest  $S/\sqrt{B}$  ratio. For example, assuming  $100 \text{ fb}^{-1}$  of integrated luminosity, in the 595 – 635 GeV range we expect 816 events in the SM, and 989 events in  $\lambda$ SUSY at the (3.1), (5.2) benchmark point, which amounts to  $6.1\sigma$  discovery significance.

In summary, we showed that the CP-odd Higgs boson of  $\lambda$ SUSY has a clear experimental signature in the  $4jl^+l^-$  channel, allowing for its discovery at the LHC with  $\sim 100 \text{ fb}^{-1}$  of integrated luminosity. Moreover, the peaked shape of the signal distribution should allow background extraction from data and an easy mass measurement. Even though the  $A \rightarrow Zh$  decay mode is less distinctive of  $\lambda$ SUSY than the  $H \rightarrow hh$  mode discussed in Section 4, its signature is much simpler and cleaner, and it could be the easiest channel to pursue when looking for  $\lambda$ SUSY signals.

## 6 Overview and conclusions

Soon the LHC will start directly probing energies well above the electroweak scale. If low-energy SUSY is the mechanism which stabilizes the gauge hierarchy, it should be discovered by the LHC experiments. However, the parameters and even the full field content of the fundamental Lagrangian will be much more difficult to determine than the existence of supersymmetric particles.



In this respect the mass of the lightest Higgs boson can be an interesting indicator. In the minimal version of supersymmetry, the MSSM, the Higgs boson is generally predicted to be light with a theoretical upper bound of around 140 GeV<sup>19</sup>. Thus the observation of an heavier Higgs boson will rule out the MSSM and all its extensions which keep couplings perturbative up to the unification scale.

A well-motivated alternative which may realize the heavy  $h$  scenario is  $\lambda$ SUSY [9]. The key feature of this model is the introduction of a chiral singlet superfield coupled to the MSSM Higgs doublets by a cubic superpotential term  $\lambda SH_1 H_2$ . Since the coupling  $\lambda$  is taken largish,  $\lambda \simeq 2$  at low energies,  $m_h$  is naturally in the range 200 – 300 GeV.

If  $\lambda$ SUSY scenario is realized in Nature, we expect early discovery of SUSY via gluino and stop decay cascades and the discovery of a SM-like lightest Higgs boson of mass around 200-300 GeV. These experimental results would be at odds with the lore of SUSY phenomenology. They are, however, very natural in  $\lambda$ SUSY.

In this paper, we have investigated how to continue the experimental study of  $\lambda$ SUSY if this puzzling picture emerges after 10 fb<sup>-1</sup> of integrated luminosity will be available. The plan is to search for the heavy neutral scalars  $H$  and  $A$ , which are expected to be in the 500 – 800 GeV range<sup>20</sup>. More specifically, we have studied a benchmark point (3.1) where  $m_H = 555$  GeV,  $m_A = 615$  GeV, while the mass of the lightest Higgs boson is  $m_h = 250$  GeV. The production cross sections of  $H$  and  $A$  are 177fb and 0.7pb, respectively, and are dominated by the gluon fusion. We have studied the discovery reach in the decay chains

$$A \rightarrow hZ \rightarrow 2VZ \rightarrow 4jl^+l^-, \quad (6.1)$$

$$H \rightarrow hh \rightarrow 4V \rightarrow 6jl^+l^-. \quad (6.2)$$

The dominant background for these signals are the diffuse  $Z4j$  and  $Z6j$  production. We suppress these backgrounds by demanding reconstruction of the vectors and the light Higgses in the intermediate state. The excess of signal events over the suppressed background allows for the heavy scalar and pseudoscalar discovery with over  $5\sigma$  significance for 100 fb<sup>-1</sup> of integrated luminosity. Moreover, we found that  $A$ 's background shape can be extracted from data, which should lead to a discovery with even less than 100 fb<sup>-1</sup>. Notice that the heavy scalar signature, relying on the  $Hhh$  coupling, is particularly distinctive of  $\lambda$ SUSY.

The masses of both  $H$  and  $A$  can be roughly determined by the position of the peaks in the total invariant mass distribution. Their masses (together with the early measurement of  $m_h$ ) will allow to determine the 3 parameters of the Higgs sector:  $m_{H^+}, \tan\beta, \lambda$  (see Section 2.1). The determination of  $\lambda$  is especially important since this coupling is the cornerstone of the  $\lambda$ SUSY hypothesis; measuring  $\lambda$  will also allow to evaluate the scale at which the non-perturbative physics sets in.

It would be interesting to find which further checks of  $\lambda$ SUSY could be performed by the LHC. The measurements of  $h$  GF production cross section could be one such check. Since  $h$  is SM-like, its production cross section in the interesting  $m_h$  range can be determined with a 10% accuracy using 100 fb<sup>-1</sup> [22, 23]. On the other hand, the theoretical uncertainty is around 20% and basically arises from the ignorance of the stop loop contribution (see Section 3.2).

---

<sup>19</sup>Assuming  $m_{\text{stop}} \lesssim 2$  TeV, see [21].

<sup>20</sup>The fourth heavy scalar, predominantly a singlet, can have a mass above a TeV and is unlikely to be observed.

Process	specific cuts	$\sigma$
$(Z \rightarrow l^-l^+)6j$	—	34.2(2) fb
$(Z \rightarrow l^-l^+)bb4j$	$p_T^l > 10$ GeV	4.22(2) fb
$(Z \rightarrow l^-l^+)cc4j$	$p_T^l > 10$ GeV	4.0(1) fb
$(Z \rightarrow l^+l^-)(t\bar{t} \rightarrow 6J)$	$\eta_l < 2.5, p_T^l > 10$ GeV	5.86(2) fb
Sum of neglected	See Appendix A	$\simeq 1$ fb + $ZV4j \lesssim 12$ fb

**Table 4:** Preliminary simulation of SM backgrounds for  $H \rightarrow l^+l^-6J$  used to select the two relevant backgrounds:  $Z6J$  and  $t\bar{t}Z$ . Apart from the shown specific cuts, all  $l^+l^-$  pairs and jets fulfill Eq. (4.4). Final state total invariant mass is between 500 and 600 GeV except for  $(Z \rightarrow l^+l^-)t\bar{t}$ , which is produced without invariant mass restrictions.

A more non-trivial test of the theory could come from the direct observation of  $H^+$ . Whether this is feasible needs a detailed study which we leave to the future.

## 7 Acknowledgements

We would like to thank R. Barbieri for carefully reading the manuscript and for useful discussions. We thank G. Corcella, F. Maltoni, M. Mangano, A. Messina for useful discussions. We also thank M. Herquet for useful advice on using MadGraph and help in using MadGraph’s cluster. The work of V.S.R. was supported by the EU under RTN contract MRTN-CT-2004-503369. V.S.R. is grateful to LPT ENS for hospitality while this work was being prepared for publication.

## A Preliminary scan of the $l^+l^-6J$ SM backgrounds

In this Appendix we describe a preliminary background scan used to select the relevant backgrounds for the  $H$  signal discussed in Section 4.5. In this scan, we computed cross sections for all SM processes with  $6Jl^+l^+$  final state using the kinematical cuts Eq. (4.4) as well as the final state invariant mass cut

$$500\text{GeV} \leq m_{tot,inv} \leq 600\text{GeV} . \quad (\text{A.1})$$

This invariant mass range, even though more narrow than the range (4.5) used in the full analysis of Sections 4.5, 4.6, covers the most important region near the  $H$  mass and is suitable to select the relevant backgrounds. The cross sections were computed either using MADGRAPH+DECAY or ALPGEN. The processes with cross section comparable or greater than the signal are those listed in Table 4. For example, the backgrounds  $ZVV2j$ ,  $ZtVj$ ,  $hh$ ,  $hV2j$ ,  $hVV$ ,  $ZVVV$  were analyzed and found to be negligibly small.  $ZVV2j$ ,  $ZV4j$  and  $h4j$  backgrounds are also negligible, although this conclusion is not immediate and relies on the use of reconstruction cuts. Below we give a more detailed discussion of these three cases.

Process	$\sigma_{n=1}$	$\sigma_{n=2}$	$\sigma_{n=3}$	$\sigma_{n=4}$
$ZWnj$	2357(3) fb	1550(3) fb	418(1) fb	$\lesssim 200$ fb
$ZZnj$	479(1) fb	280(2) fb	67.2(4) fb	$\lesssim 30$ fb

**Table 5:**  $ZVnj$  cross sections. The last column is an extrapolation obtained taking  $\frac{1}{2} \left( \frac{\sigma_{n=1}}{\sigma_{n=2}} + \frac{\sigma_{n=2}}{\sigma_{n=3}} \right)$  as a naïve suppression factor for the step from  $n = 3$  to  $n = 4$ .

### A.1 $h4j$

A full matrix element calculation of this process summing over gluon fusion(GF) and vector boson fusion(VBF) is not available. Separate computations of GF and VBF are available in MADGRAPH, and GF is also available in ALPGEN. We used the faster ALPGEN for the GF case, although it has a caveat that all jets are assumed light and at least one has to be a gluon. Enforcing cuts Eq. (4.4), setting  $\mu_F^2 = m_h^2 + \sum_j p_T^j{}^2$ , and with no final state invariant mass restrictions we got

$$\sigma(gg \rightarrow hg3j) = 253(1) \text{ fb.} \quad (\text{A.2})$$

The VBF was computed with MADGRAPH by setting the  $ggh$  effective coupling to zero. For  $\mu_F^2 = m_Z^2$  and with no final state invariant mass restrictions we got a cross section a factor of 5 smaller than (A.2). We concluded that the GF process alone should give a reasonable estimate for the total cross section, and in particular that it is consistent to neglect interference effects.

We thus proceeded to generate a sample of  $hg3j$  events using the ALPGEN GF process. Then, using DECAY, the  $h$  was made to decay into  $l^+l^-jj$ . Enforcing cuts Eqs. (4.4), (4.7) and (A.1) yields  $\sigma = 0.42(2)$  fb, at this stage comparable with the signal (see Eq. (4.3)). We then subjected this sample to the reconstruction cuts R1 and R2 discussed in Section 4.6. The rejection efficiency was found to be  $\sim 1/30$ , reducing this background to a level which can be safely neglected.

### A.2 $ZVV2j$

We will only discuss  $ZWW2j$ , which is the largest of the  $ZVV2j$  backgrounds. Its cross section after cuts Eq. (4.4) and Eq. (A.1) was computed through ALPGEN and amounts to 4.33(2) fb. Decaying the Zs into leptons and Ws into quarks, we get

$$\sigma(pp \rightarrow 2j4Jl^+l^-) = 0.2 \text{ fb.}$$

This already looks negligible, but for reasons which will be clear in the next section we generated a sample and computed the rejection efficiency for the reconstruction cuts R1 and R2 of Section 4.6. The found rejection efficiency was  $\sim 1/50$ , making this background completely negligible.

### A.3 $ZV4j$

Simulation of this process with a generic matrix element generator like MADGRAPH would require computational resources out of our reach. At the same time we are not aware of any specialized

code simulating this process. For this reason we resorted to an order-of-magnitude estimate for this background, which seems to indicate that it is subleading.

First of all, we simulated  $ZWnj$  and  $ZZnj$  in ALPGEN until  $n = 3$  (the current limit). Enforcing production cuts Eq. (4.4) and Eq. (A.1) we obtained the results given in Table 5. Conservatively extrapolating these numbers, we got an estimate  $\sigma(ZV4j) \lesssim 230$  fb. Making the Z and W decay, we get

$$\sigma(pp \rightarrow ZV4j \rightarrow 2j4Jl^-l^+) \lesssim 11 \text{ fb.} \quad (\text{A.3})$$

quite a bit higher than the signal total cross section of Eq. (4.3). However, the background is reducible, and we would like to estimate the rejection efficiency for the reconstruction cuts R1 and R2 of Section 4.6. We cannot produce a sample of  $ZV4j$ , but we can use the intuitively clear fact that  $ZV4j$  is more reducible than  $ZWW2j$  analyzed in the previous section. Thus we expect that the rejection efficiency should not be worse than 1/50 found for  $ZWW2j$ . From (A.3), this gives  $\sigma \lesssim 0.21$  fb for the events which passed the reconstruction cuts. Comparing this bound with values reported in Table 2 we conclude that adding this channel would enhance the total background cross section by no more than 20%. As such, this would not change the conclusion about the observability of  $H$ .

## References

- [1] LEP Electroweak Working Group, as updated on <http://www.cern.ch/LEPEWWG>
- [2] R. Barbieri, L. J. Hall and V. S. Rychkov, “Improved naturalness with a heavy Higgs: An alternative road to LHC physics,” *Phys. Rev. D* **74**, 015007 (2006) [arXiv:hep-ph/0603188];  
F. D’Eramo, “Dark matter and Higgs boson physics,” arXiv:0705.4493 [hep-ph];  
R. Enberg, P. J. Fox, L. J. Hall, A. Y. Papaioannou and M. Papucci, “LHC and Dark Matter Signals of Improved Naturalness,” arXiv:0706.0918 [hep-ph].
- [3] J. R. Ellis, J. F. Gunion, H. E. Haber, L. Roszkowski and F. Zwirner, “Higgs Bosons in a Nonminimal Supersymmetric Model,” *Phys. Rev. D* **39**, 844 (1989);  
M. Masip, R. Munoz-Tapia and A. Pomarol, “Limits on the mass of the lightest Higgs in supersymmetric models,” *Phys. Rev. D* **57**, 5340 (1998) [arXiv:hep-ph/9801437].
- [4] M. Bastero-Gil, C. Hugonie, S. F. King, D. P. Roy and S. Vempati, “Does LEP prefer the NMSSM?,” *Phys. Lett. B* **489**, 359 (2000) [arXiv:hep-ph/0006198].
- [5] P. Batra, A. Delgado, D. E. Kaplan and T. M. P. Tait, “The Higgs mass bound in gauge extensions of the minimal supersymmetric standard model,” *JHEP* **0402**, 043 (2004) [arXiv:hep-ph/0309149];
- [6] Raising Higgs mass in SUSY with perturbative unification:  
J. R. Espinosa and M. Quiros, “Gauge unification and the supersymmetric light Higgs mass,” *Phys. Rev. Lett.* **81**, 516 (1998) [arXiv:hep-ph/9804235];  
K. Tobe and J. D. Wells, “Higgs boson mass limits in perturbative unification theories,” *Phys. Rev. D* **66**, 013010 (2002) [arXiv:hep-ph/0204196];  
A. Maloney, A. Pierce and J. G. Wacker, “D-terms, unification, and the Higgs mass,” *JHEP* **0606**, 034 (2006) [arXiv:hep-ph/0409127];

- K. S. Babu, I. Gogoladze and C. Kolda, “Perturbative unification and Higgs boson mass bounds,” arXiv:hep-ph/0410085.
- [7] Raising Higgs mass in theories with low SUSY breaking scale:  
N. Polonsky and S. Su, Phys. Lett. B **508**, 103 (2001) [arXiv:hep-ph/0010113];  
J. A. Casas, J. R. Espinosa and I. Hidalgo, ‘The MSSM fine tuning problem: A way out,’ JHEP **0401**, 008 (2004) [arXiv:hep-ph/0310137].
  - [8] Fat Higgs models: R. Harnik, G. D. Kribs, D. T. Larson and H. Murayama, “The minimal supersymmetric fat Higgs model,” Phys. Rev. D **70**, 015002 (2004) [arXiv:hep-ph/0311349];  
S. Chang, C. Kilic and R. Mahbubani, “The new fat Higgs: Slimmer and more attractive,” Phys. Rev. D **71**, 015003 (2005) [arXiv:hep-ph/0405267];  
A. Delgado and T. M. P. Tait, “A fat Higgs with a fat top,” JHEP **0507**, 023 (2005) [arXiv:hep-ph/0504224];  
A. Birkedal, Z. Chacko and Y. Nomura, “Relaxing the upper bound on the mass of the lightest supersymmetric Higgs boson,” Phys. Rev. D **71**, 015006 (2005) [arXiv:hep-ph/0408329].
  - [9] R. Barbieri, L. J. Hall, Y. Nomura and V. S. Rychkov, “Supersymmetry without a light Higgs boson,” Phys. Rev. D **75**, 035007 (2007) [arXiv:hep-ph/0607332].
  - [10] B. Gripaios and S. M. West, “Improved Higgs naturalness with or without supersymmetry,” Phys. Rev. D **74**, 075002 (2006) [arXiv:hep-ph/0603229].
  - [11] See, e.g., P. Gambino and M. Misiak, Nucl. Phys. B **611**, 338 (2001) [arXiv:hep-ph/0104034];  
M. Neubert, Eur. Phys. J. C **40**, 165 (2005) [arXiv:hep-ph/0408179].
  - [12] S. Mizuta and M. Yamaguchi, “Coannihilation effects and relic abundance of Higgsino dominant  $LSP_s$ ,” Phys. Lett. B **298**, 120 (1993) [arXiv:hep-ph/9208251].
  - [13] S. Dimopoulos and G. F. Giudice, “Naturalness constraints in supersymmetric theories with nonuniversal soft terms,” Phys. Lett. B **357**, 573 (1995) [arXiv:hep-ph/9507282]. A. G. Cohen, D. B. Kaplan and A. E. Nelson, “The more minimal supersymmetric standard model,” Phys. Lett. B **388**, 588 (1996) [arXiv:hep-ph/9607394].
  - [14] S. I. Bitukov and N. V. Krasnikov, “The LHC (CMS) discovery potential for models with effective supersymmetry and nonuniversal gaugino masses,” Phys. Atom. Nucl. **65**, 1341 (2002) [Yad. Fiz. **65**, 1374 (2002)] [arXiv:hep-ph/0102179]; S. I. Bitukov and N. V. Krasnikov, “LHC (CMS) SUSY discovery potential for nonuniversal gaugino and squark masses and the determination of the effective SUSY scale,” arXiv:hep-ph/0210269.
  - [15] W. M. Yao *et al.* [Particle Data Group], J. Phys. G **33**, 1 (2006).
  - [16] W. Beenakker, R. Hopker, M. Spira and P. M. Zerwas, “Squark and gluino production at hadron colliders,” Nucl. Phys. B **492**, 51 (1997) [arXiv:hep-ph/9610490].
  - [17] M. Spira, Higlū: A program for the calculation of the total higgs production cross section at hadron colliders via gluon fusion including qcd corrections, hep-ph/9510347.
  - [18] <http://people.web.psi.ch/spira/proglist.html>
  - [19] V. Barger, T. Han and D. G. E. Walker, “Top quark pairs at high invariant mass: A model-independent discriminator of new physics at the LHC,” arXiv:hep-ph/0612016.

- [20] A. Djouadi, “The anatomy of electro-weak symmetry breaking. I: The Higgs boson in the standard model,” arXiv:hep-ph/0503172.
- [21] A. Djouadi, The anatomy of electro-weak symmetry breaking. II: The Higgs bosons in the minimal supersymmetric model, **hep-ph/0503173**.
- [22] ATLAS Collaboration, ATLAS detector and physics Performance Vol. 2. No. ATLAS TDR 15, CERN/LHCC 99-15.
- [23] CMS Collaboration, CMS Physics Technical Design Report - Volume II: Physics Performance. No. CERN/LHCC 2006-021.
- [24] F. Maltoni and T. Stelzer, MadEvent: Automatic event generation with madgraph, *JHEP* **02** (2003) 027 [**hep-ph/0208156**].  
J. Alwall *et al.*, arXiv:0706.2334 [hep-ph].  
T. Stelzer and W. F. Long, Comput. Phys. Commun. **81**, 357 (1994) [arXiv:hep-ph/9401258].
- [25] M. Bowen, Y. Cui and J. D. Wells, “Narrow trans-TeV Higgs bosons and  $H \rightarrow h h$  decays: Two LHC search paths for a hidden sector Higgs boson,” *JHEP* **0703**, 036 (2007) [arXiv:hep-ph/0701035].
- [26] <http://root.cern.ch>
- [27] <http://root.cern.ch/root/AtIfast.html>
- [28] ATLAS Collaboration, ATLAS detector and physics Performance Vol. 1. No. ATLAS TDR 14, CERN/LHCC 99-14.
- [29] M. L. Mangano, M. Moretti, F. Piccinini, R. Pittau and A. D. Polosa, Alpgen, a generator for hard multiparton processes in hadronic collisions, *JHEP* **07** (2003) 001 [**hep-ph/0206293**].  
M. L. Mangano, M. Moretti and R. Pittau, collisions: W b Nucl. Phys. B **632**, 343 (2002) [arXiv:hep-ph/0108069].  
F. Caravaglios, M. L. Mangano, M. Moretti and R. Pittau, Nucl. Phys. B **539**, 215 (1999) [arXiv:hep-ph/9807570].
- [30] CDF Collaboration, Measurement of the inclusive jet cross section in  $Z(\rightarrow ee) + jets$  production, *CDF note 8827*.
- [31] D0 Collaboration, Z+jet production in the d0 experiment: A comparison between data and the pythia and sherpa monte carlo, *D0 note 5066-CONF*.